

Supplemental Figures

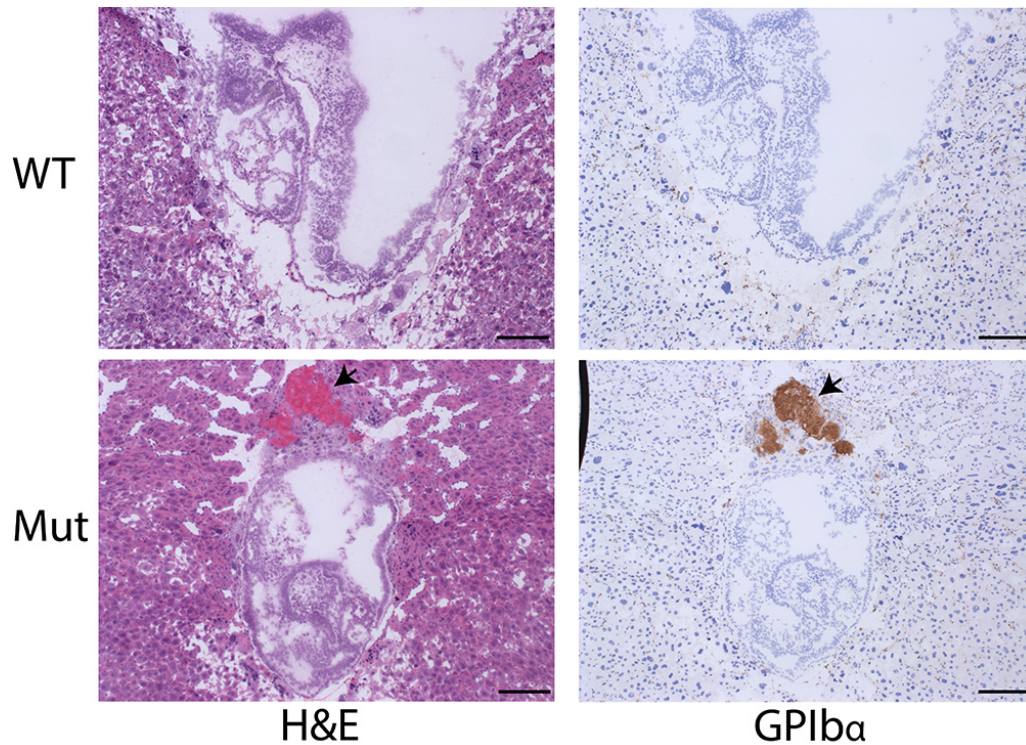


Figure S1. **Deposited material juxtaposed to the ectoplacental cone at E8.5 immunostains with antibody to platelet surface marker GPIb α (brown) consistent with identification as a fibrin/platelet clot, related to Figure 1.** Sections of implantation sites for *Pcolce*^{-/-} E8.5 embryos found to be wild type (WT) or homozygous for a mutation (Mut), at the *Wbscr16* locus (both embryos were on a C57BL/6 background) were stained with H&E, or with antibody to the platelet GPIb α marker. The early embryonic lethal phenotype included appearance of a fibrin/platelet-containing clot juxtaposed to the embryonic (anti-mesometrial) pole of E7.5 conceptuses, and then appearance of a larger clot deposited at the extraembryonic (Mesometrial) pole, juxtaposed to the ectoplacental cone and parietal yolk sac placenta at E8.5. Mutant embryos were small and apparently growth-restricted, with disappearance of the embryonic space, normally filled with amniotic fluid, compaction of the embryo proper, and apparent replacement of much of the ectoplacental cone with fibrin and platelets. Scale bars 100 μ m.

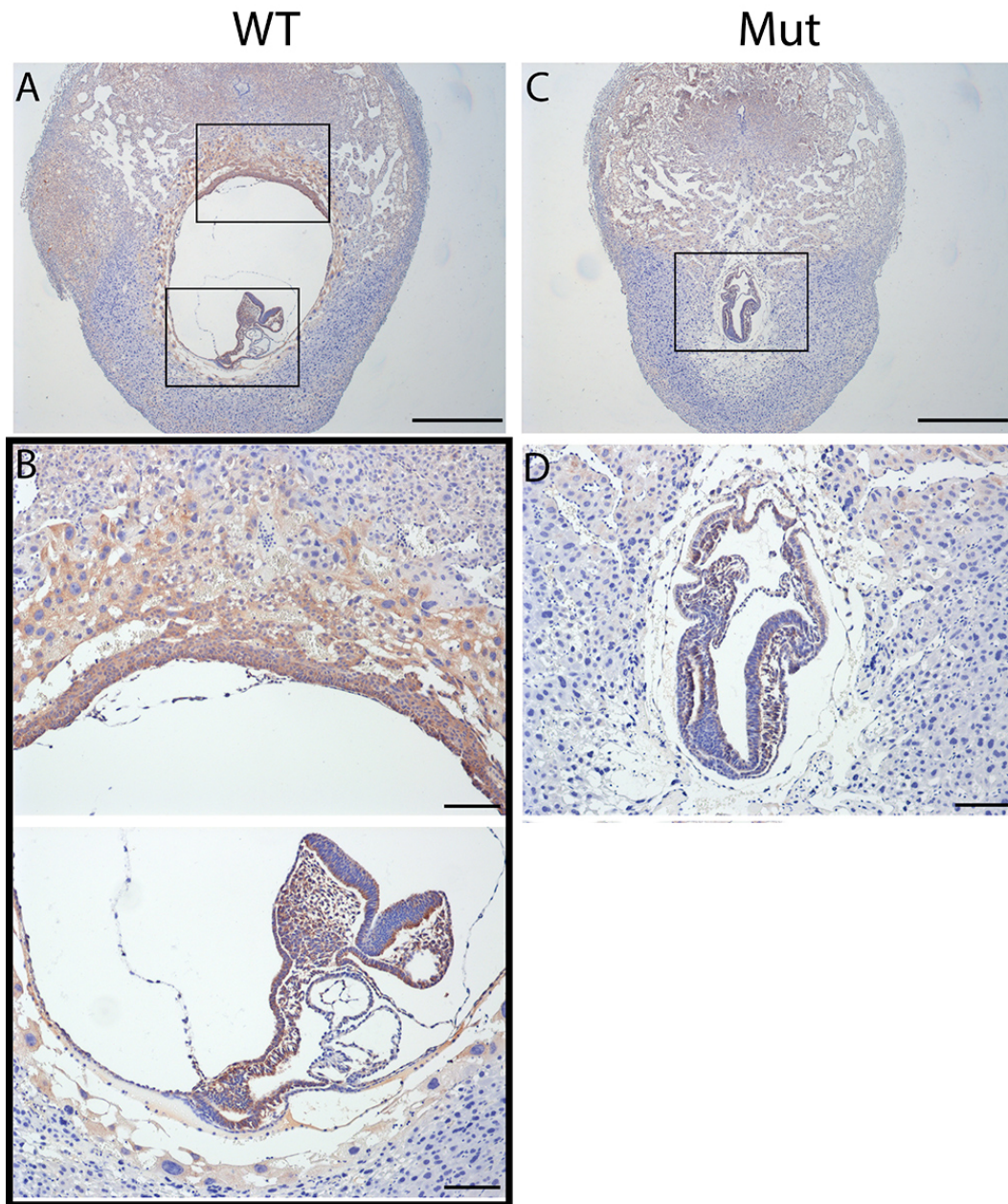


Figure S2. WBSCR16 is broadly expressed at E8.5 and is readily detected in HeLa cells, related to Figure 1. Immunohistochemical staining with anti-WBSCR16 antibody (NOVUS) showed WBSCR16 protein to be broadly distributed in (A and B) WT yolk sac placenta, decidua, and embryo, with highest levels found in the TGCs and ectoplacental cone (a source of TGC precursor cells) at E8.5, and thus in affected structures at the time that the lethal phenotype occurs. (C and D) Mutant WBSCR16 was also detectable, albeit at relatively low levels, in placenta, decidua, embryo, and aberrant TGCs, showing mutant WBSCR16 to be at least to some degree stable. The boxed areas in A and C (scale bars 600 μm) are shown at higher magnification in B and D (scale bars 100 μm), respectively. (E) A western blot shows WBSCR16 to be readily detected as a doublet in HeLa cells lysed with RIPA buffer containing EDTA-free protease inhibitors (Roche), and detected on blots with rabbit anti-WBSCR16 polyclonal antibody (1:1000, Abcam).

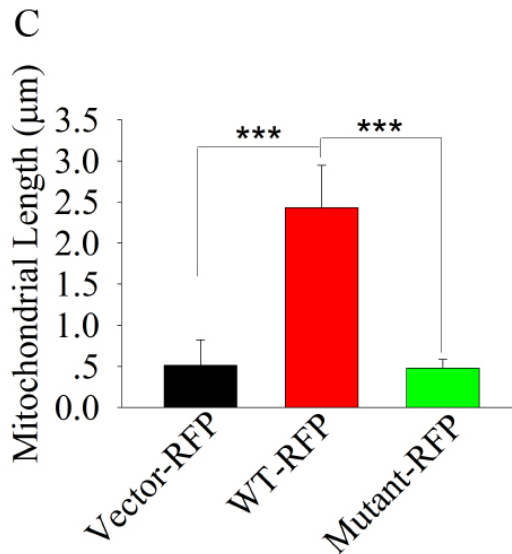
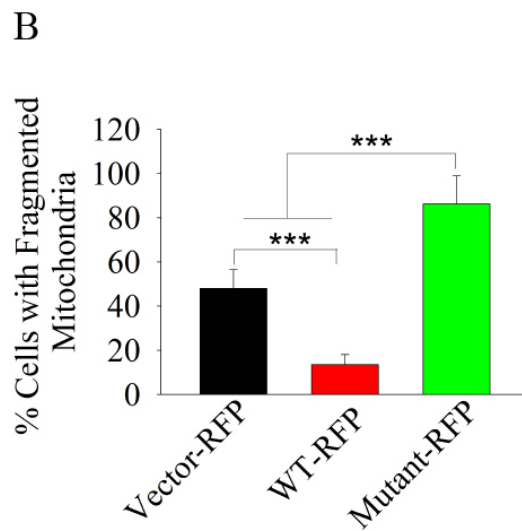
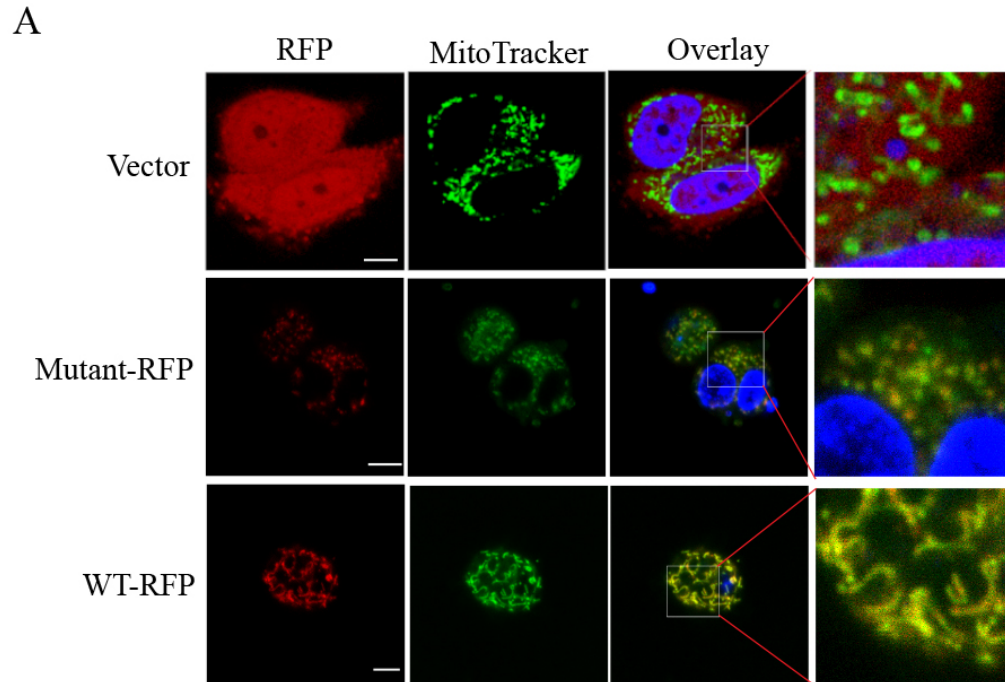
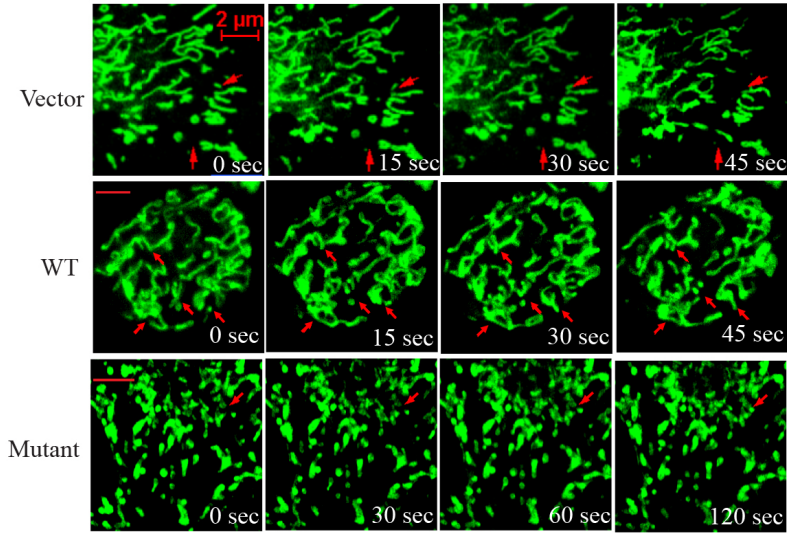


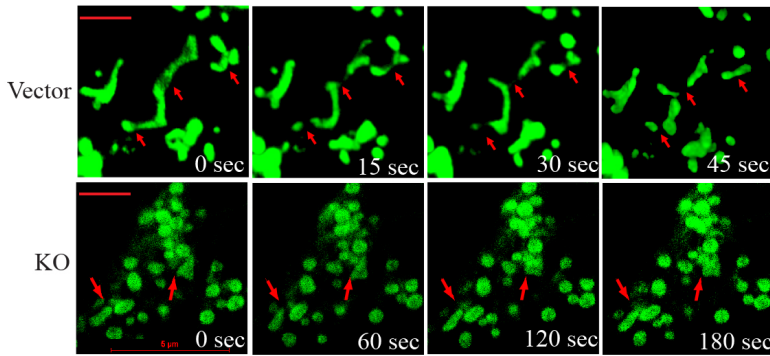
Figure S3. In HeLa cells in which WBSR16 has been knocked out by CRISPR-Cas9, mitochondrial fusion is rescued by overexpression of RFP-tagged wild type, but not mutant WBSR16, or by empty vector expressing RFP only (Vector), related to Figure 2.

Enlargements of boxed areas of overlay results (column 4) more clearly show rescue of fusion upon wild type WBSR16-RFP overexpression. Scale bars 5 μm . Quantification is shown for percentage of cells with fragmented mitochondria (B) and for mitochondrial length (C). For panel B, > 20 cells were scored from each set of cells transfected with a particular vector. For panel C, 10 mitochondria were measured per cell, for a total of > 20 cells per set of cells transfected with a particular vector.

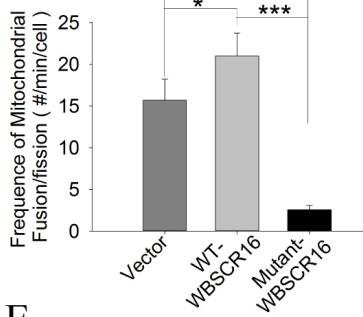
A



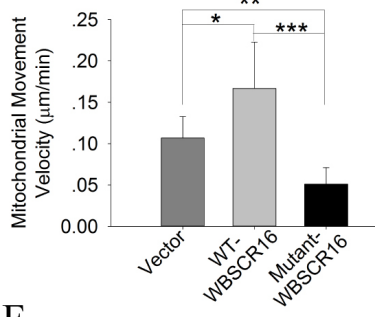
B



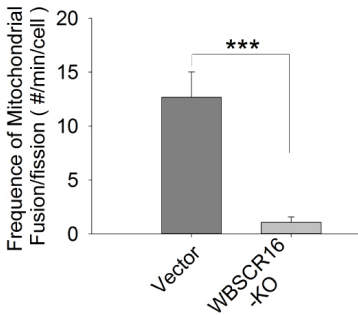
C



D



E



F

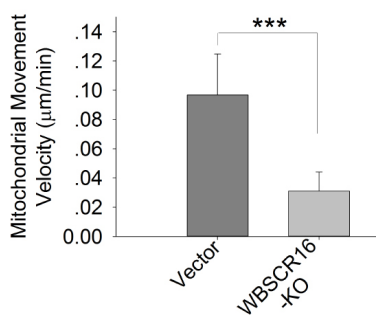


Figure S4. Effects of WBSCR16 mutation or ablation on mitochondrial dynamics, related to Figure 2 and to movies 1 and 2. Still frames are shown from time-lapse confocal microscopy. (A) HeLa cells were transfected with vector overexpressing wild type (WT) or mutant WBSCR16, or with corresponding empty vector (Vector). (B) HeLa cells were transfected with vector containing WBSCR16-specific sequences for CRISPR-Cas9 knockout (KO), or with corresponding empty vector. All cells were stained with MitoTracker Green 36 hours post transfection. In empty vector or WT-WBSCR16 transfected cells in *A* and *B*, mitochondria were highly motile and fusion/fission events were frequent. In contrast, mitochondrial motility and fission/fusion events were much reduced in cells transfected with mutant-WBSCR16 vector or subjected to CRISPR/Cas9 WBSCR16 knockout. *A* and *B* are still frames of Movies S1 and S2, respectively. Mitochondria in WT-WBSCR16 overexpression cells had higher fusion and fission frequencies than those in empty vector-transfected cells (Movies S1 and 2). Quantification is shown for the frequency of mitochondrial fusion/fission events, in #/min/cell (C and E) and for movement velocity, in $\mu\text{m}/\text{min}$ (D and F) for the cells of panel A (C and D) and of panel B (E and F). For quantifying frequencies of mitochondrial fusion/fission events, >20 cells were tracked per group, and for quantifying mitochondrial movement velocity, >20 representative mitochondria were tracked per group, with subsequent averaging of data. Data are presented as mean \pm S.D. Quantification employed Nikon NIS-Elements software.

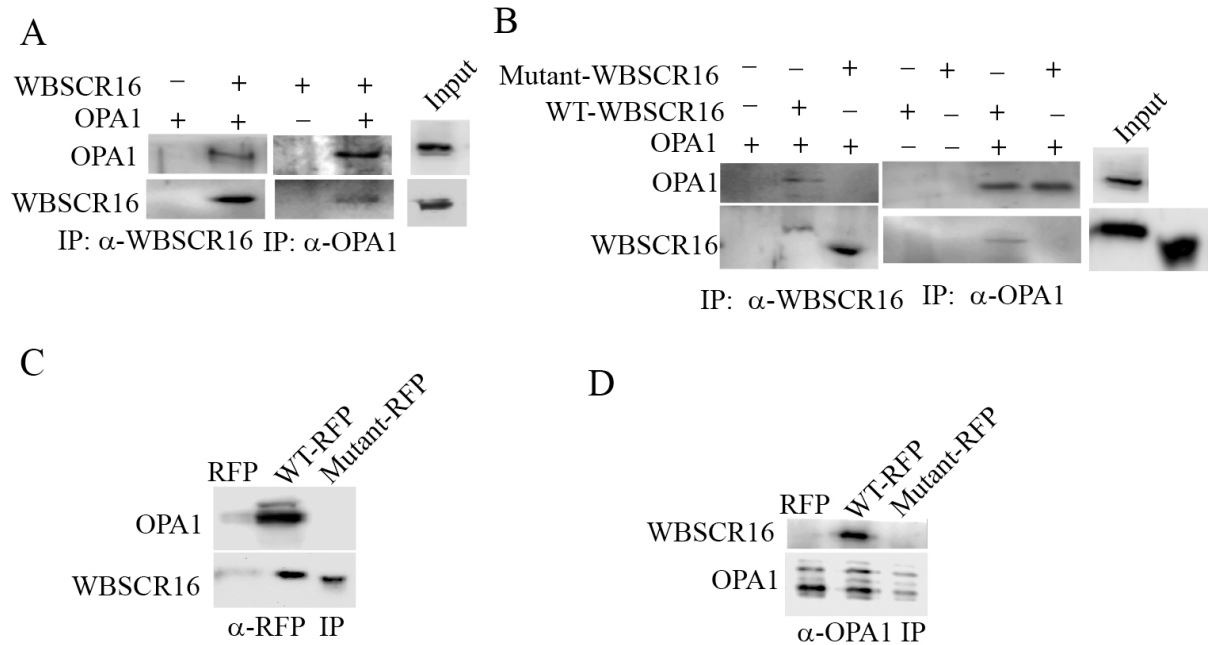


Figure S5. **Binding of wild type, but not mutant WBSCR16 with OPA1, related to Figures 2 and 5.** (A) Immunoblots show that *in vitro* immunoprecipitation (IP) of FLAG-tagged WT WBSCR16 with anti-FLAG antibody pulled down OPA1, and that immunoprecipitation of OPA1 pulled down WBSCR16 as well. OPA1 was not FLAG-tagged. (B) *In vitro* immunoblots from another set of pull-down experiments show that although OPA1 pulls down WT WBSCR16 and vice versa, it does not pull down, nor is it pulled down by, mutant wBSCR16. Immunoblots of input WT and mutant recombinant WBSCR16 are also shown. (C and D) Immunoblots are shown of immunoprecipitations from lysates of HeLa cells transfected for expression of either WT or mutant WBSCR16. The immunoprecipitations employed either anti- red fluorescent protein (RFP) antibody (C) or antibodies to OPA1 (D).

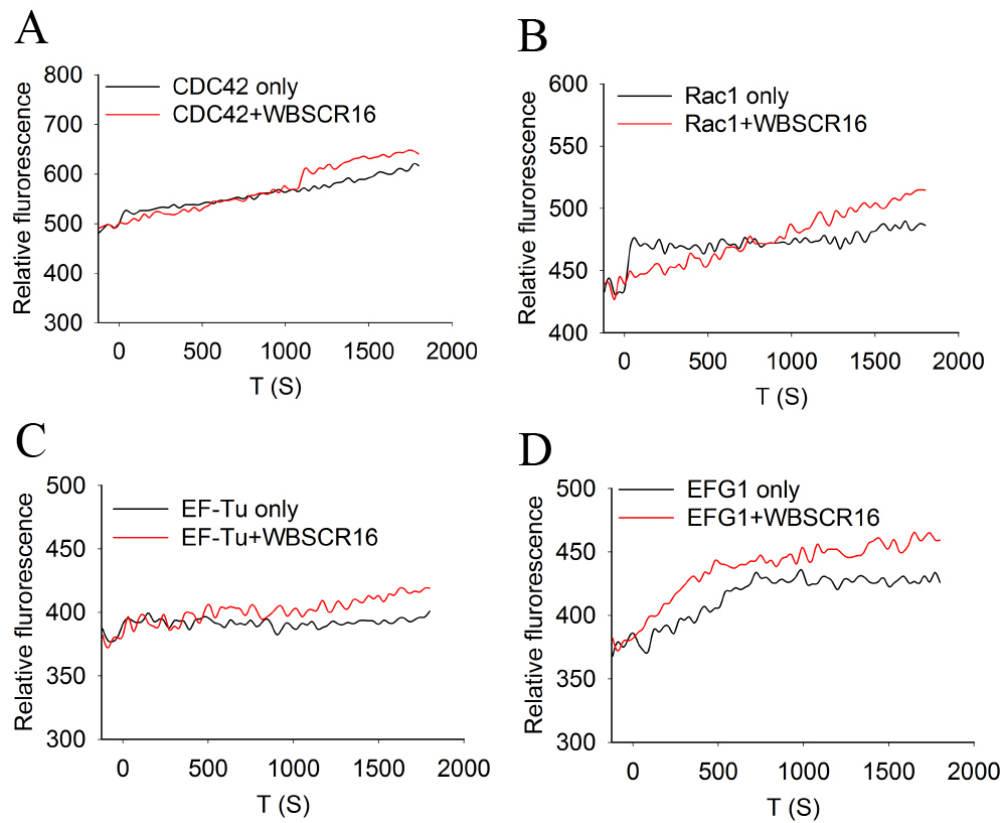


Figure S6. **WBSR16 is not a GEF for CDC2, Rac1, EF-Tu, or EFG1, related to Figure 5.** A fluorescent assay for GEF activity (loading of mant-GTP onto GTPases) shows a lack of GEF activity of WBSR16 for CDC42 (A), Rac1 (B), EF-Tu (C), and EFG1 (D).

Table S1. Length of cell cycle duration* in WT and WBSR16^{-/-} HeLa cells, related to Figure 3.

Genotype	G ₁	S	G ₂ /M	Total
WT	4	6	5	15
KO	15	6	8	29

*All durations are given in hours.

Supplemental Experimental Procedures

Genetic Mapping, Deep Sequencing, and Animal Care

The mild *Pcolce*^{-/-} phenotype on a Black Swiss background, but early embryonic lethality on a C57BL/6 (B6) background suggested the presence of a second locus (locus^C) in the latter background that strongly contributed to the phenotype, either by modifying *Pcolce* function or independently. 1% of *Pcolce*^{-/-} B6 mice were “escapers”, suggesting rare recombination events occurring in a relatively small distance separating *Pcolce* and locus^C. Mapping of locus^C was begun by crossing a Black Swiss *Pcolce*^{-/-} male with B6 *Pcolce*^{+/-} females, yielding *Pcolce*^{-/-} and *Pcolce*^{+/-} progeny. As all F1 progeny were heterozygous for Black Swiss/B6 alleles at all loci, the presence of F1 *Pcolce*^{-/-} progeny indicated that a single copy of the Black Swiss allele at locus^C was sufficient to confer viability on *Pcolce*^{-/-} embryos. *Pcolce*^{-/-} F1 mice were then backcrossed to B6 *Pcolce*^{+/-} heterozygotes and N2 neonates were genotyped. Of 328 N2 neonates, 102 were *Pcolce*^{-/-}, and DNA of the latter was used to map locus^C by identifying genomic regions with decreased average homozygosity for B6 SNPs (for loci with no phenotypic effect, average homozygosity would be 0.5). As genetic data on the Swiss Black strain is not publically available, we identified SNPs between the parental Black Swiss and B6 backgrounds via the Affymetrix Mouse Diversity Array (Jax Mouse Diversity Genotype Array Service). *Pcolce*^{-/-} N2 had decreased heterozygosity at two SNPs on Chromosome (Chr) 5 (rs31753463 at 45 cM and rs6249331 at 90 cM) with the B6 alleles present at a frequency of 0.16 and 0.31 respectively. While 2-point linkage analysis did not definitively show linkage between either marker and locus^C (for rs31753463 LOD_{max} = 2.49 and rs6249331 LOD_{max} = 2.63, respectively), it did indicate that locus^C could be located between 45 and 80 cM on Chr 5. As *Pcolce* is within this region (at 76 cM), locus^C would be linked to *Pcolce*, if also within this region. To verify linkage, a second cross was performed: a Black Swiss *Pcolce*^{+/+} male with a number of B6 *Pcolce*^{+/-} females, to produce *Pcolce*^{+/-} progeny in which the *Pcolce* null allele and surrounding genetic region was contributed by the B6 parent. *Pcolce*^{+/-} F1 mice were then backcrossed to B6 *Pcolce*^{+/-} heterozygotes and subsequent N2 neonates were genotyped. The 6% N2 *Pcolce*^{-/-} neonates observed was significantly less than the 20% expected if locus^C had segregated independently of *Pcolce* (chi-square test, $p=0.0006$), verifying linkage, and placing locus^C within the 45 to 80 cM Chr 5 region. Importantly, 10 generations of backcrossing Black Swiss *Pcolce*^{-/-} mice with B6 mice newly purchased from Harlan labs (thus not raised in our lab) yielded a proper Mendelian ratio of viable *Pcolce*^{-/-} B6 pups, indicating the lethality-causing polymorphism at locus^C to be a spontaneous mutation that appeared during the original backcrosses between *Pcolce*^{-/-} Black Swiss mice X B6 mice reared in our lab (thus not a modifier gene endogenous to the B6 strain).

With available SNPs, we were unable to narrow the 45 to 80 cM region further. To obtain additional informative markers we performed deep sequencing of the DNA of *Pcolce*^{-/-} mice on Black Swiss and B6 backgrounds (the B6 background was the one on which the *Pcolce*^{-/-} genotype is embryonic lethal) at 10X coverage (Illumina HiSeq2000). Sequencing results were aligned with the reference mouse genome (Bowtie software and SAMtools). 931 homozygous polymorphisms were identified in the mutant B6 background that were not known common variants or present in the Black Swiss background. To ensure that the causative mutation was not missed, the region of interest was expanded to cover 50 cM to either side of *Pcolce1* (from 40 to 151 Mb, the latter of which is at the end of Chr 5), which encompassed the 45 to 80 cM region. Only one polymorphism was within the coding sequence of a gene in this region:

chr5.mm10:g.134163662C>T (NM_033572.2:c.922G>A), resulting in a Glu to Lys substitution in *Wbscr16*. Mapping, using polymorphisms between the mutant B6 and Black Swiss backgrounds, further narrowed the region containing the causative mutation to a 4.6 Mb span, 1.5 Mb upstream of *Pcolce1*. This span included *Wbscr16* and no additional polymorphisms in either coding or noncoding (genic or intergenic) sequences. Subsequent matings to separate the *Pcolce*-null and *Wbscr16* mutant alleles confirmed homozygosity for the latter to be sufficient to produce early lethality.

All mice were housed and treated in accordance with NIH guidelines, using protocols approved by the Research Animal Resources Center of the University of Wisconsin-Madison.

Histology and Immunohistology

Pregnant females were sacrificed at 8.5 dpc, and embryos were dissected from uteruses, fixed with formalin and paraffin embedded. For placental lactogen 1 (PL-1) staining, 5 μ m sections were stained with hematoxylin and eosin (H&E) or with a goat anti-PL-1 antibody (1:50, Santa Cruz) after 5 min treatment with proteinase K, at 37°C, followed by treatment with 0.4% Triton for 10 min at room temperature. Primary antibody was incubated at room temperature for 2.5 h and secondary antibody, rabbit anti-goat tagged with horseradish peroxidase (Bio-Rad, 1:1000), was incubated for 1 h at room temperature.

For WBSR16 staining, paraffin embedded sections were probed with rabbit anti-human WBSR16 (1:20, Novus Biologicals). Sections were deparaffinized and antigen retrieval was performed using sodium citrate. Primary antibodies were incubated overnight at 4°C and secondary antibody, goat anti-rabbit HRP conjugated (1:1000, Bio-Rad), was incubated 1 h at room temperature. For GPIIb α staining, frozen sections were air dried and fixed with 100% acetone. Primary rat anti-mouse GPIIb α antibody (1:250, emfret ANALYTICS) was incubated 2 h at room temperature and the secondary antibody, goat anti-rat tagged with horseradish peroxidase (1:1000, Bio-Rad), was incubated 1 h at room temperature.

Plasmid Construction and Recombinant Proteins

RNA was extracted from skeletal muscle of wild type mice and mice heterozygous for the *Wbscr16* mutation with TRIzol (Life Sciences Technology). 1 μ g RNA was reverse transcribed using oligo(dT) nucleotides and SuperScript (Invitrogen). *Wbscr16* coding sequences were then PCR amplified using 5'-ATAAGCGGTTGAGGCGTGAC-3' forward and 5'-GGCTTTGTCCACACACCTCT-3' reverse primers. A single 1458 bp product was produced from wild type cDNA, but 1458 bp and ~1300 bp products were produced from heterozygous mutant cDNA. Amplicons were sub-cloned into pGEM-T (Promega). Sequencing of *Wbscr16* heterozygous mutant cDNA clones revealed fifteen of fifteen 1458 bp clone inserts to correspond to wild type *Wbscr16*, and fifteen of fifteen 1300 bp clone inserts to contain the Glu308Lys *Wbscr16* substitution and 164 bp deletion.

Wild type and mutant WBSR16 sequences were PCR amplified from pGEM-T clones in a two-step process. Step one employed primers 5'-ACAAGCTTATGGCGGCGCCATAAGCGGTTGAGG-3', forward (to add a HindIII site and missing GCC triplet at the 5' end of WBSR16 sequences), and 5'-AGCGGTACCGTGATGAATGACTTGGCTAGAG-3', reverse (to add a KpnI site at the 3' end of the insert). In the second step, the same reverse primer was used, but the forward primer was 5'-ACAAGCTTATGCCATAAGCGGTTGAGGCG-3', to add an additional GGCGGC of missing N-terminal WBSR1 sequences. Inserts were then inserted between the HindIII and

KpnI sites of pTagRFP-N (Evrogen). These constructs and WBSCR16 CRISPR/Cas9 plasmids (Santa Cruz Biotechnology), were transfected into mammalian cells with TransIT-LT1 reagent (Mirus). For figure 2C, WBSCR16 was knocked out via CRISPR/Cas9, followed 3 days later by FACS sorting for GFP expression. Cells were then transfected with empty vector, or vectors expressing RFP-tagged WT or mutant WBSCR16. 36 h later, cells were stained with MitoTracker Green.

N-terminal FLAG-tagged recombinant WBSCR16, for *in vitro* experiments was produced from human WBSCR16 sequences that had been codon optimized, synthetically generated and subcloned into pFastBacI by GeneArt. Protein was produced in Sf9 insect cells and purified on an anti-FLAG M2 (Sigma) affinity column. The *in vitro* GEF assay was performed using kit BK100 (Cytoskeleton), employing the manufacturer's protocol. Recombinant human proteins purchased for *in vitro* assays were: N-terminal His-tagged Cdc42 (Cat. # CD01), Rac1 (Cat. # RC01), and Dbs GEF domain (Cat. #GE01) (Cytoskeleton); and C-terminal MYC/DDK tagged MFN1 (Cat. # TP307184), MFN2 (Cat. # TP302218), and OPA1 (Cat. # TP311417) (OriGene).

Cell Culture and Imaging

Mfn1^{-/-}, *Mfn2*^{-/-}, *Mfn1/2*^{-/-}, and *OPA1*^{-/-} MEFs^{11, 19} and HeLa cells were obtained from ATCC. In live-cell experiments, cells were plated on collagen coated 14 mm glass bottom dishes (MatTek, USA). After incubation with 100 nM MitoTracker (Cell Signal), cells were imaged in live cell imaging solution (ThermoFisher) on the 37°C preheated stage of a Nikon A1RS confocal microscope. Cells were imaged with an oil immersion PlanApo 60X objective and appropriate laser lines for each fluorophore were used. For time-lapse confocal microscopy, mitochondrial dynamics were recorded for 10 min at 15-sec intervals.

Cell Proliferation and Apoptosis Assays

Cell proliferation was measured via mitochondrial dehydrogenase reduction of tetrazolium salt (3-(4,5-dimethylthiazol-2-yl)-2,5-diphenylterazolium bromide; MTT) assay, with OD readouts at 570 nm. For apoptosis assays, floating cells in medium and trypsinized adherent cells were harvested, combined, and fixed in 70% ethanol. Cells were then treated with RNase A (200 µg/ml) for 1 h prior to propidium iodide (PI, 50 µg/ml) staining. DNA content was detected by flow cytometry using a FACSCalibur flow cytometer (Becton Dickinson) and percent of cells with sub-G₁ DNA content (apoptotic cells) was determined.

In addition to the above, floating cells were harvested and combined with adherent cells for extraction with SDS-loading buffer. Samples were then boiled and subjected to SDS-PAGE and immunoblotting with antibody (1:1000, Cell Signaling) for cleaved caspase 3.

Assays of transfected cells were performed 36 h post transfection.

Cell Cycle Analysis of WBSCR16-ablated HeLa Cells

HeLa cells, transfected with empty vector or with vector containing WBSCR16-specific sequences for CRISPR-Cas9 knockout were stained 36 h later with Hoechst 33342 (2 µg/ml and 30 min incubation at 37°C), sorted by FACS into G₁-, S-, and G₂/M-phase cells, then released into culture medium. Cells were then harvested at different time points, fixed with 70% ethanol, and incubated with 200 µg/ml RNase A and 50 µg/ml propidium iodide at 37 °C for 30 min, for DNA profiling (Fig. S5). FACS was via FACSCalibur flow cytometer and data were analyzed with FlowJo software.

Mitochondrial Lysis and Immunoprecipitation Assays

Mitochondria were isolated, as described below, and then lysed with RIPA buffer containing EDTA-free protease inhibitors (Roche) and 25 units of alkaline phosphatase (NEB) per ml cell lysate. After 30 min incubation on ice, samples were centrifuged 10 min at 12,000 g, at 4 °C. Supernatants were then incubated overnight at 4 °C with anti-MFN1, -MFN2 (Origene), -OPA1 (cell signaling) or -WBSCR16 (Abcam) antibodies coupled to Aminolink Resin (Pierce Direct IP kit, Thermo Scientific). The resin was then washed three times and eluted, following manufacturer's instructions, and resin/antibody-bound proteins were subjected to SDS-PAGE and immunoblotting.

For *in vitro* pull down assays of recombinant proteins, 50 ng WBSCR16 was preincubated 3 h at 4 °C with/without 100 ng of OPA1 (Origene, NM_130832) in 50 mM Tris-HCl, pH 7.5, 150 mM NaCl, 2.5 mM MgCl₂, 0.1% Triton X-100, and 1 mg/ml BSA, followed by overnight incubation with OPA1 antibodies coupled to Aminolink resin. Alternatively, 50 ng OPA1 was preincubated 3 h at 4 °C with/without 100 ng of WBSCR16 in 50 mM Tris-HCl, pH 7.5, 150 mM NaCl, 2.5 mM MgCl₂, 0.1% Triton X-100, and 1 mg/ml BSA, followed by overnight incubation with WBSCR16 antibodies (Abcam) coupled to Aminolink resin. Immunoprecipitates were washed, eluted and subjected to SDS-PAGE and immunoblotting, as above.

***In vitro* GEF exchange Assay**

Assays were carried out with the RhoGEF Exchange Assay Biochem Kit (BK100, Cytoskeleton). Briefly, 4.5 µl of 5 µM GTPase was added to 7.5 µl of 2x exchange reaction buffer (40 mM Tris pH 7.5, 100 mM NaCl, 20 mM MgCl₂, 1.5 µM mant-GTP) in 384 well plates. Plates were then read immediately (excitation 360 nm, emission 440 nm). After 5 readings (for a total of 150 seconds), 3 µl of 2.5 µM WBSCR16, hDbs, or dH₂O, was added to wells, with an immediate resumption of reading (60 readings for a total of 30 min). Three independent assays were performed, each in triplicate. V_{max} and exchange rate values were calculated following the manufacturer's recommended protocol. V_{max} (AFU/Sec) and exchange rates (µmol mant-GFP/µmol GEF/Sec), respectively, were: WBSCR16-OPA1, 1.01, 1.87×10^{-3} ; WBSCR16-MFN1, 0.18, 0.46×10^{-3} ; WBSCR16-MFN2, 0.19, 0.57×10^{-3} ; Dbs-CDC42, 1.94, 2.13×10^{-3} ; Dbs-Rac1, 0.175, 0.43×10^{-3} . All GEF exchange assays were performed with purified recombinant proteins, described above in the "Plasmid Construction and Recombinant Proteins" section.

GTPase Activity Assays. Assays were carried out with the GTPase/ATPase ELIPA Biochem Kit (BK051, Cytoskeleton). For Figure 4E, 200 ng GTPase, WBSCR16, or Dbs was diluted in 50 µl ELIPA reaction buffer (15 mM PIPES, pH 7.0; 5 mM MgCl₂) in 96-well microtiter plates. Then another 50 µl ELIPA reaction buffer containing 1 mM GTP with/without 200 ng WBSCR16 or Dbs was added to the wells. For the WBSCR16 concentration dependent assay of Figure 4F, serial 400, 200, 100, 50, 25, and 12.5 ng amounts of WBSCR16 were diluted in 50 µl ELIPA reaction buffer containing 1 mM GTP, which were then added to 96-well microtiter plates already containing 200 ng MFN1, MFN2, or OPA1, each diluted in 50 µl ELIPA reaction buffer.

Assays were incubated 2 h at room temperature, mixed well with another 100 µl ELIPA mixture comprising 24 parts ELIPA reagent 1 (2-amino-6-mercapto-7-methylpurine riboside):1.25 parts ELIPA reagent 2 (Purine nucleotide phosphorylase), and 100 parts ELIPA reaction buffer. Thirty minutes later, plates were spectrophotometrically analyzed in a plate

reader at 360 nm.

Subfractionation of mouse liver mitochondria

Mouse liver mitochondria were isolated essentially as described (Frezza et al., 2007). Briefly, mouse liver was rinsed with ice-cold IB_c buffer (10 mM Tris-MOPS, 1 mM EGTA, 20 mM sucrose, pH 7.4), minced, homogenized, and centrifuged twice at 600 g for 10 min at 4 °C. Supernatant was transferred to another tube and centrifuged at 7,000 g for 10 min to obtain mitochondria. After washing with IB_c buffer, mitochondria were subfractionated by a modification of the procedure of Hovius et al. (Hovius et al., 1990). Briefly, mitochondrial pellets were suspended in 10 mM KH₂PO₄ (pH 7.4), incubated 15 min, diluted 2-fold with buffer B (32%(w/v) sucrose, 30% glycerol (v/v), 10 mM MgCl₂ in 10 mM KH₂PO₄, pH 7.4) and incubated another 15 min. The pellet was sonicated twice for 15 s with 1-min intervals at 60-70 watts, and then centrifuged at 12,000 g for 10 min at 4 °C. The supernatant was loaded onto a discontinuous sucrose gradient (51.3, 37.7, 25.3% w/v, 2 ml each) in 10 mM KH₂PO₄, pH 7.4; and centrifuged 3 h at 210,000 g in a Beckman SW 41 Ti rotor. Four fractions were collected: Top supernatant (intermembrane space, IS); 25.3/37.7% interface membrane protein (outer membrane, OM); and the 37.7/51.3% interface membrane protein (inner membrane, IM) fractions were diluted 3-fold in buffer A (250 mM mannitol, 0.5 mM EGTA, 5 mM Hepes, pH 7.4). The bottom pellet (inner membrane plus matrix, IMM) was either resuspended in buffer A, or resuspended in buffer B, diluted 2-fold with 10 mM KH₂PO₄ (pH 7.4), for further sonication. The additional sonication was 5 times, 15 s each, with 1-min intervals, at 60-70 watt. This additional sonication was followed by centrifugation at 12,000 g for 10 min at 4 °C. The sonication supernatant was then loaded onto a 2 ml discontinuous sucrose gradient and centrifuged, as above. The supernatant from this gradient contained soluble matrix proteins (MX), while the pellet contained the “2nd IM” fraction of inner membrane purified away from soluble matrix proteins. Proteins of each of the fractions described above were collected at 16,000 g for 10 min at 4 °C, resuspended in SDS loading buffer, and subjected to immunoblotting.

To determine the orientation of WBSR16 bound to the mitochondrial inner membrane, mitoplasts were prepared and subjected to immunoprecipitations both before and after lysis, essentially as described (Tokarska-Schlattner et al., 2008). Briefly, purified mitochondria were suspended in isotonic buffer A, containing 0.1% (w/v) bovine serum albumin and protease inhibitors (cOmplete, Roche) on ice for 15 min with 0.3 mg digitonin/mg protein. After washing 3 times with buffer A by 5 min centrifugation at 10,000 X g, mitoplasts were resuspended in buffer A with antibodies coupled to Aminolink Resin (Thermo Fisher), for 1 h at 4 °C. Antibodies were then recovered, following the manufacturer’s protocol, rinsed three times with RIPA buffer (150 mM NaCl, 50 mM Tris-HCl, pH7.5, 1% NP-40, 0.5% deoxycholic acid, 0.1% SDS, 1 mM phenylmethylsulfonyl fluoride and protease inhibitors), and suspended in Laemmli buffer. After washing 3 times in buffer A to remove unbound antibodies, the intact mitoplasts were then suspended in RIPA buffer containing Aminolink coupled- antibodies, and lysed mitoplasts were incubated 1 h at 4 °C. Antibodies linked to resin were then recovered, rinsed 3 times with RIPA, and suspended in Laemmli buffer.

Study of Neurons from heterozygous mutant *Wbscr16* Mice

Meninges and blood vessels were removed from neonatal hippocampus in cold Hank's balanced salt solution. After rinsing with cold high glucose DMEM (HGDMEM), brains were dissociated with papain (2.5 mg/ml, 30 min at 37°C), with cell suspensions passed through a 100 µm cell strainer. Centrifuged (7,000 g for 5 min) cells were then resuspended in HGDMEM, 10% fetal bovine serum, followed by plating on poly-D-lysine-coated cover slips. Cells were switched to neurobasal B27 medium after 5 h of plating, and after 48 h were treated with 1 µM Ara-c, for 48 h. Cells were then maintained in neurobasal B27 medium. Mitochondrial membrane potential was measured by staining with potentiometric fluorescence dye TMRM, as described (Joshi and Bakowska, 2011). For fragmentation assays, cells were labeled 30 min with 250 nM MitoTracker green dye and time lapse imaging was performed to observe mitochondrial morphology before and after 50 µM glutamate exposure. Mitochondrial aspect ratio (length /width) was calculated by averaging thousands of mitochondria from multiple images, in an unbiased way (using overall, rather than region-specific fields), using NIH imageJ software. After color thresholding, the mitotracker images were binarized and subjected to particle analysis to obtain the aspect ratio.